

Characterisation of high energy electron irradiation damage in UPt_3 samples

P. Rodière^{†‡}, J.P. Brison[‡], A.D. Huxley[†], F. Rullier Albenque[‡], and J. Flouquet[†]

[†] *Département de Recherche Fondamentale sur la Matière Condensée,
SPSMS, CEA-CENG, 38054 Grenoble-Cedex 9, France*

[‡] *H.H. Wills Laboratory of Physics University of Bristol Tyndall Avenue Bristol, BS8 1TL U.K.*

[‡] *CRTBT, CNRS, 25 avenue des Martyrs, BP166, 38042 Grenoble Cedex 9, France*

[‡] *SPEC, Ormes des Merisiers, CEA, 91191 Gif sur Yvettes, France*

We present transport and specific heat measurements on high quality single crystals of UPt_3 before and after irradiation by high energy electrons. We observe a strong dependence of the critical temperature with the sample thickness. The dramatic effects of the irradiation on the specific heat in the superconducting state can then be simply explained in terms of an inhomogeneous distribution of superconducting transition temperatures. The question of the failure of the "universal limit" in the heat transport of UPt_3 is reexamined, and the conditions for a clean experimental test are established.

PACS numbers:

I. INTRODUCTION

Unconventional superconductors are mainly found among strongly correlated electronic systems, where impurities seem to be dominantly in the unitary limit¹. In such a case, even a very small concentration of defects will induce a finite density of states at zero energy². Moreover, a finite impurity concentration induces conduction bands which contribute to transport properties³: for example, impurities should add a linear term in temperature (T) to the thermal conductivity for $T \rightarrow 0$. More subtle effects were predicted depending on the particular gap topology. If a line of nodes is present on the Fermi surface, and in presence of defects, the linear term of the thermal conductivity should be universal (i.e. independent of the impurity concentration) for a small variation of T_c ^{4,5}. This is considered as a very robust test of the unconventional nature of the superconducting state and of its gap topology.

Such a universal limit has been observed in a few quasi-2D unconventional superconductors such as $\text{YBa}_2\text{Cu}_3\text{O}_{6.9}$ ⁶, $\text{Bi}_2\text{Sr}_2\text{CaCu}_2\text{O}_8$ ⁷ and Sr_2RuO_4 ⁸. But it failed in the underdoped High- T_c compound $\text{YBa}_2\text{Cu}_4\text{O}_8$ ⁹. In this last case, the origin of the absence of the universal limit is still not clear, and could be attributed among others to the nature of the superconductivity or the particular ground state of this compound. Further investigations have to be done in compounds where the electronic ground state is well established. Moreover, the universal limit has never been observed in any three dimensional unconventional superconductor.

One of the best studied unconventional 3D superconductor is the heavy fermion UPt_3 . Its superconducting state is particularly interesting because it exhibits a well known phase diagram^{10,11}, each phase corresponding to a different symmetry of the superconducting gap. Various scenarios exist for these phases¹², corresponding to different types of nodes of the superconducting gap. Probing the universal limit in the different crystallographic direc-

tions would be a very strong test of the models⁵.

Impurity effects in UPt_3 have been studied in many different ways. Substitution of Uranium or Platinum by another element have been used to study the decrease of the critical temperature^{13,14,15}, and the interplay between the magnetism and the superconductivity¹⁶. They would not be appropriate to probe the universal limit due to the rapid change of the normal state properties and T_c with even the smallest concentrations that can be reasonably studied. Small defect concentrations can be tuned with annealing, which varies the number of intrinsic metallurgical defects. A main advantage of annealing is the possibility to follow the effects on the same sample. Its influence on physical properties at low temperature like the specific heat¹⁷ or transport properties¹⁸ has been reported. Nevertheless, it does not seem appropriate to investigate a possible universal limit in UPt_3 due to the small range of change of the critical temperature and the lack of knowledge of the nature of the defects: extended defects are expected rather than point defects, and they may require more involved descriptions¹⁸ which spoil the strength of the theoretical predictions.

A third technique uses high energy electron irradiation damage to create point defects¹⁹. It seems ideal for such studies, combining the advantages of the previous techniques: the vacancy and interstitial defects created by electron irradiation have a size of a few Ångströms, small compared to the coherence length of UPt_3 ($\xi_0 \approx 100\text{Å}$); Moreover, it is possible to access a wide range of defect concentrations simply by tuning the irradiation time. Finally, the same sample can be studied for the various concentrations, and a simple annealing at 700°C suppresses again all defects, refreshing the sample. This technique has been used in UPt_3 to study the influence of impurities on T_c , on the upper critical field H_{c2} and on the thermal conductivity at very low temperature¹⁹. No "universal limit" has been observed, a surprising result given the fact that the thermal conductivity of the pure sample is perfectly understood with the most popular scenarios^{20,21} which predict a universal behaviour

at least in the basal plane. But measurements of the specific heat of irradiated samples already indicated a very unexpected behaviour, with a large broadening of the transition²². Theoretical investigations of the specific heat broadening due to the natural (gaussian) dispersion of defect concentrations²³ cannot explain the importance of the effect observed, and further experimental characterisation of the induced disorder seemed necessary.

In this paper, we present new results on the specific heat and transport measurements of UPt_3 samples damaged by high energy electrons. We show that the sample thickness has a dramatic influence on the results, explaining the previous failure of the measurements¹⁹. We give quantitative estimates of the distribution of defects in the sample, and determine the conditions for a clean test of the universal limit in this system. The experimental procedure and the main results are described in section II. In section III, an introduction to the creation of defects by electron irradiation is presented. Section IV presents a phenomenological model used to describe quantitatively our results. In the last sections, the previous results are briefly discussed in the framework of our description.

II. EXPERIMENTAL DETAILS AND MAIN RESULTS

Pure samples were cut from the same single crystal grown under ultra-high vacuum by the Czochralski method. The shape of the sample for resistivity measurements was a bar of typical length 5 mm and width 0.23 mm. The samples R1, R2 and R3 have been thinned down to 190, 90 and 70 μm respectively, in order to probe the depth of the irradiation damage. R4 and R5 with a respective thickness of 220 μm and 240 μm were prepared to study the evolution of the normal state transport properties for different rates of irradiation. R1 and R4 were cut with the electrical current along the c-axis, R2, R3 and R5 with the electrical current in the basal plane. The two samples measured by specific heat (C1 and C2) were plates 270 μm thick and a surface roughly $2 \times 2 \text{ mm}^2$. After being cut and/or thinned, all samples were annealed under ultra high vacuum ($< 3.10^{-10}$ Torr) at 950°C during 5 days. The quality of the resistivity samples has not been altered by the thinning process since the three samples exhibited a high critical temperature T_c of 0.55 K (R1) and 0.56 K (R2 and R3).

The irradiations by high energy electrons have been performed in the low temperature facility of the Van der Graaff accelerator of the "Laboratoire des solides irradiés" of Ecole Polytechnique at Palaiseau (France). The resistivity samples were held next to each other on a thin fibre glass plate with GE varnish. The thinnest dimension was parallel to the electron beam. This plate was wrapped in a thin copper foil, held rigidly inside a liquid hydrogen bath. The three samples were irradiated

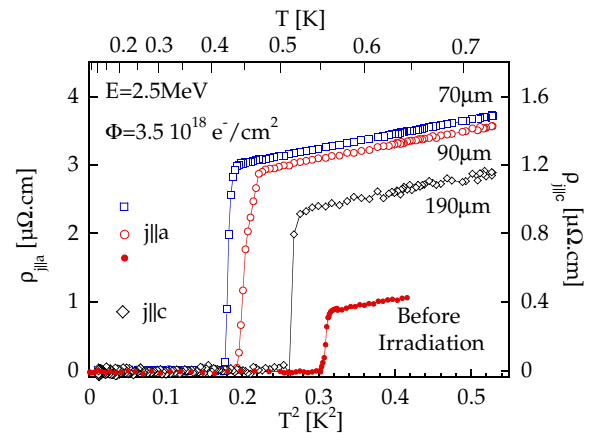


FIG. 1: Temperature dependence of the resistivity of the three samples of UPt_3 , R1 R2 and R3 (with a thickness of respectively 190, 90 and 70 μm) after an irradiation by electrons of energy of 2.5 MeV with a fluence of $3.5 \cdot 10^{18} \text{ e}^-/\text{cm}^2$. The sample R2 is also shown before irradiation (closed circles) and is typical of pure samples of UPt_3 . The current is oriented along the a-axis except for sample R1 (c-axis). The left scale respects the ratio of the anisotropy of the effective mass of the quasi-particles observed in pure samples (2.5).

simultaneously, and they remained well within the homogeneous region of the electron beam. Electrical contacts on the samples were done with silver paste (solder might have reannealed part of the defects), removed before, and made again after the irradiation. The samples C1 and C2 for the specific heat measurements were wrapped directly the thin copper foil, and were irradiated separately. Incident electrons were accelerated at an energy of 2.5 MeV for samples for resistivity measurements and C1, and with an energy of 1.5 MeV in the case of sample C2. The irradiation takes place in liquid hydrogen. Two Faraday cups located in the front and behind the samples are used to estimate the irradiation fluence at the level of the sample²⁴. The electron flux is limited to $\sim 10^{14} \text{ e}^-/\text{cm}^2/\text{s}$ in order to avoid the heating of the sample during irradiation. Fluences (Φ) between 1.8 and $13.9 \times 10^{18} \text{ electron/cm}^2$ (e^-/cm^2) have been used. After irradiation, the samples were warmed up to room temperature and transferred in different experimental set-ups to perform resistivity and specific heat measurements. This procedure results in some annealing of the defects created at low temperature.

The resistivity measurements have been performed with a traditional four wires technique with a 17 Hz AC-current bridge. The specific heat measurements have been performed with a semi adiabatic technique. All samples have been measured before and after irradiation.

When electrons go through the matter, a part of their energy is lost via inelastic collisions with the target electrons. Typically, the energy loss is of the order of 1-2 keV/ μm ²⁵. In the case of 100-200 μm thick the energy loss can be as high as 400 keV. But as long as the energy

transferred to the target nucleus, which depends on the atomic weight of the nucleus and on the incident energy of the electron, is much larger than the minimum energy required to displace it (threshold energy), the cross section for the atomic displacement does not depend drastically on this energy. So, in this case, the decrease of the electron energy through the target compound will not induce strong inhomogeneities in the damage distribution. However, if the energy transferred to the target nucleus is close to the threshold energy, one could expect that the decrease of the incident energy along the path induces that electrons will not be longer able to displace atoms in the whole thickness of the samples. In this latter case the critical temperature can be expected to change differently along the electron path depth. We suspect that this situation could explain the large broadening of the specific heat transition observed previously on irradiated UPt_3 samples²². In order to test this assumption, we have performed two kinds of measurements : (i) we have used lower energy electrons (if close to the threshold, the irradiation effects should then be drastically reduced), and (ii) we have measured irradiated samples of various thicknesses in order to check a possible dependence of T_c with thickness.

Figure 1 shows the result of the last test. It displays the resistivity of the three samples of different thickness, irradiated during the same experiment and with the same fluence $\Phi = 3.5 \times 10^{18} \text{e}^-/\text{cm}^2$. The most striking result is that indeed, the thinner the sample, the stronger the drop in T_c . This correlation between sample thickness and T_c change is a direct proof of the inhomogeneity of the irradiation damage. As regard the normal state properties, the temperature dependence of the resistivity remains quadratic ($\rho(T) = \rho_0 + A.T^2$) for all samples. Both terms ρ_0 and A increase under irradiation, and again, ρ_0 increases more strongly when the sample is thinner. However, A is closer to the value of a pure sample when the irradiated sample is thinner. We take this as pointing to an increased average disorder for thinner samples and a wider distribution of defects for thicker samples. We shall make these conclusions more quantitative in section V.

Figure 2 presents the effects of irradiation at two different energies on the specific heat. The top panel compares virgin sample C2, and the same sample irradiated with a fluence of $4.5 \times 10^{18} \text{e}^-/\text{cm}^2$ at 1.5 MeV : within experimental accuracy, there is no effect at all of the irradiation, both in the normal and superconducting state. The simplest interpretation is that with an incident energy of 1.5 MeV, the transmitted energy to the uranium and platinum atoms is below the threshold energy for defect formation. These results at 1.5 MeV should be contrasted with the bottom panel of figure 2. It shows the drastic effects at 2.5 MeV²² on sample C1, with a new measurement at a low fluence of $1.8 \times 10^{18} \text{e}^-/\text{cm}^2$. The virgin sample C1 (like C2) exhibits the well known double specific heat jump at temperatures (defined by an onset criteria) of $T_{c+} = 550 \text{ mK}$ and $T_{c-} = 498 \text{ mK}$ respectively.

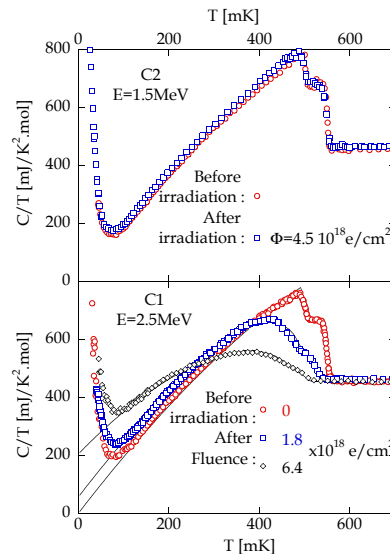


FIG. 2: Temperature dependence of the specific heat of the same sample of UPt_3 before (open circle) and after damaged by irradiations. The irradiations were performed with incident electrons at an energy of 1.5 MeV (top panel sample C2) and 2.5 MeV (bottom panel sample C1). The top panel demonstrate that at 1.5 MeV, no effects are observed on the specific heat (no defects creation). On the bottom panel, the line for the sample before irradiation is a phenomenological description of the specific heat behaviour with a small homogeneous distribution of T_c of 16 mK. After irradiation, a good fit in the whole temperature range and for the two fluence is obtained with an exponential decrease of the rate of defects in the depth of the sample (see text). The exponential distribution is characterised by the length $\lambda = 90 \mu\text{m}$ and the decrease of T_c for an infinitely thin sample by the parameter $dT_c/d\Phi = -115 \text{ mK}/10^{18} \text{e}^-/\text{cm}^2$.

Both transitions show only a small broadening of 16 and 12 mK respectively, demonstrating the very good quality of the sample. Note that at very low temperature the strong upturn in the specific heat already reported²⁶ is well observed. The origin of this upturn could be a magnetic ordering transition but is not directly connected to the superconducting state. In the following analysis this upturn will be ignored. After irradiation, the same sample shows a strong broadening of the specific heat : the two superconducting transitions are already hardly distinguishable for a fluence of $1.8 \times 10^{18} \text{e}^-/\text{cm}^2$, and are totally smeared at a higher fluence.

By contrast, the onset critical temperature shifts only very little, much less than observed by resistivity on thin samples (R3 for example). From this point of view, the irradiation effects are different from the annealing effects where broadening and T_c decrease are intimately correlated¹⁷. It points again to an inhomogeneous distribution of point defects. Let us note that normal state properties are little affected by irradiation (apart from a smaller mean free path). Indeed, above the superconducting transition, the sample exhibits a clear

linear dependence of the specific heat ($C = \gamma T$) with a large value of the Sommerfeld coefficient γ characteristic of the heavy fermion Fermi liquid regime. The irradiations do not affect this Fermi liquid behaviour nor the value of γ . They are also reversible : the original specific heat has been recovered after a subsequent annealing at 700°C during 5 days under ultra high vacuum.

III. CREATION OF DEFECTS BY HIGH ENERGY ELECTRON IRRADIATION

We have stated that the experimental behaviours of the resistivity and the specific heat suggest that 2.5 MeV is very close to the energy necessary to create stable defects in UPt₃. In this section, we will present a short introduction to the creation of defects by high energy electron irradiation with a special emphasis to the special case of UPt₃. A plausible qualitative explanation of the origin of such inhomogeneities is proposed. We then develop a simple model and introduce a characteristic length of defect creation which allows us to describe phenomenologically and quantitatively the broadening of the specific heat transition. This model is then applied to the resistivity results.

The process of defect creation in a sample irradiated by high energy electrons is based on elastic collisions between the incident electrons and the atomic nuclei of the crystal²⁷. There is an activation energy - the threshold energy E_t - necessary to create stable vacancy-interstitial defects (Frenkel pairs), i.e. vacancy and interstitial separated enough to avoid spontaneous recombination. In the case of monoatomic hexagonal compact structures, E_t is typically about a few ten eV²⁷. This value has to be compared to the maximum energy transferred to the atom by an incident electron which is inversely proportional to the mass of the nuclei. In UPt₃, Uranium and Platinum are heavy nuclei with $Z=238$ and $Z=195$ respectively. The maximum transmitted energy is respectively of 79.5 and 97.0 eV for incident electrons of energy 2.5 MeV, and 34.1 and 41.7 eV for an incident energy of 1.5 MeV. Therefore the fact that irradiation with 1.5 MeV electrons has no effect on the specific heat gives us a bottom limit for the threshold energies in UPt₃ equal respectively to 34.1 and 41.7 eV for U and Pt atoms. These values are quite high and might be explained by the high compactness of the crystallographic structure in UPt₃.

The cross section for displacement of an atom by an electron with an incident energy E depends both on the threshold energy and on the energy transferred to the atoms. For thick samples, it is then necessary to take into account the energy losses along the electron path. It is found to be equal to -2.37 keV/ μ m and to remain approximately constant over a depth of 270 μ m (corresponding to the thickest sample of this study). This decrease of incident energy as a function of the penetration depth inside the sample induces a decrease

of the cross section for elastic collisions and therefore of the concentration of defects. This is a schematic mechanism from which the rate of defects creation depends on the depth inside the sample. It is even stronger if the initial energy is barely enough for the transmitted energy to exceed the threshold. A detailed rigorous description of rate of defect creation inside the sample as a function of energy is certainly possible. Such analyses have been effectively performed, for example to determine the threshold energies in the diatomic compound TaC²⁴. But it is not our purpose here, which is rather, first, to check that this is indeed responsible for the measured effects and, second, to determine which experimental conditions have to be used in order to prevent such an inhomogeneous distribution. This is the aim of the phenomenological model developed in the next section.

IV. PHENOMENOLOGICAL MODEL

In order to quantify our hypothesis, we need the concentration of defects as a function of depth in the sample ($c(x)$, $x = 0$ corresponding to the side of the sample facing directly the incident beam). As explained above, $c(x)$ which is of course proportional to fluence, is not known exactly and depends on parameters like the energy dependence of the cross section and the decrease of the energy of the incident electrons due to inelastic scattering. So we have chosen to use a simple phenomenological exponential dependence, parameterised by a characteristic length for defect creation λ : $c(x) = c(0)exp(-x/\lambda)$.

The second element is the relationship between defects concentration and T_c decrease. This is well known and studied, both experimentally and theoretically. Indeed, it has been already demonstrated that the critical temperature of UPt₃ is strongly dependent on the concentration of defects^{13,14,18}. This feature is common to all unconventional superconductors like high- T_c oxides (see for example²⁸) or Sr₂RuO₄²⁹. The decrease of the critical temperature in a conventional or unconventional superconductor due to a pair breaking mechanism is always described by the Abrikosov-Gor'kov formula³⁰:

$$\ln \left(\frac{T_c}{T_{c0}} \right) = \psi \left(\frac{1}{2} \right) - \psi \left(\frac{1}{2} + \frac{\alpha}{2\pi k_B T_c} \right) \quad (1)$$

T_c is the critical temperature, T_{c0} the critical temperature of the sample without pair breaking, ψ the digamma function and α characterises the strength of the pair breaking mechanism. In the limit of small pair breaking ($\alpha \rightarrow 0$), the decrease of the critical temperature is linear and equal to $\frac{\pi\alpha}{4k_B}$. Larkin has shown that for an unconventional superconductor with isotropic impurity scattering, α is equal to $\frac{\hbar\Gamma}{2}$ where Γ is the scattering rate³¹. At fixed incident energy E , for an infinitely thin

sample, the scattering rate is proportional to the number of defects and therefore to the fluence. As the cross section of individual scattering centers is not known, we rather define a new parameter : $\left| \frac{dT_c}{d\Phi}(E) \right|$, the initial rate of decrease of T_c with fluence, for an infinitely thin sample. For a given material, this parameter will only depend on the (fixed) incident energy. Then, the local critical temperature $T_c(x)$ at depth x in the sample is given by equation (1) with :

$$\alpha = \alpha(x) = -\frac{4k_B}{\pi} \left| \frac{dT_c}{d\Phi}(E) \right| \Phi \exp(-x/\lambda) \quad (2)$$

A strong test of the model is to reproduce the specific heat behaviour. Again, exact calculations of the specific heat for a given homogeneous concentration of defects are possible³². They depend on the symmetry of the order parameter, but they do not account for the double transition. So we used a much simpler approach, which appears more proportionate to the ambition of our model. We first make a simple fit of the specific heat of the virgin sample, which defines a function $C_{T_{c0}}(T)$ which respects the entropy conservation. For a homogeneous sample of reduced temperature T_c (due to an *homogeneous* distribution of pair breaking centers), the specific heat will be $C_{T_c}(T)$. It has a residual linear term, due to impurity bound states². This term is estimated crudely as $\gamma_{res} = \left. \frac{C(T)}{T} \right|_{T \rightarrow 0} = \gamma \frac{T_{c0} - T_c}{T_{c0}}$, where γ is the Sommerfeld coefficient in the normal state. We then simply rescale with respect to T_c the specific heat of the virgin sample, using the following expression which respects entropy balance :

$$\frac{C_{T_c}(T)}{T} = \gamma_{res} + \frac{\gamma - \gamma_{res}}{\gamma} \frac{C_{T_{c0}}(T \frac{T_{c0}}{T_c})}{T \frac{T_{c0}}{T_c}} \quad (3)$$

A simple integration over the sample thickness using equations 3, 2 and 1 gives the fit of the specific heat of irradiated samples for each fluence, which depends only of the two free parameters λ and $\left| \frac{dT_c}{d\Phi}(E) \right|$. On figure 2, the full lines are the results of the fit for $\lambda = 90 \mu\text{m}$ and $\left| \frac{dT_c}{d\Phi}(2.5\text{MeV}) \right| = 115 \text{mK}/10^{18} \text{e}^- \cdot \text{cm}^{-2}$. It is gratifying to see that it reproduces well both the broadening and the small shift of the onset critical temperature for both fluences and with the same parameters. More insight into the physical effects at work is gained looking at the distribution of T_c inside the sample deduced from these parameters.

Let us first discuss the T_c change as measured by resistivity. As soon as a thin layer of the sample is superconducting, it will short circuit the sample. In the present geometry of the irradiation, the part of the sample with the largest critical temperature (producing the drop to the zero resistivity on figure 1) is the side opposite to the electron beam. It should be the same part of the sample that gives the onset T_c for the

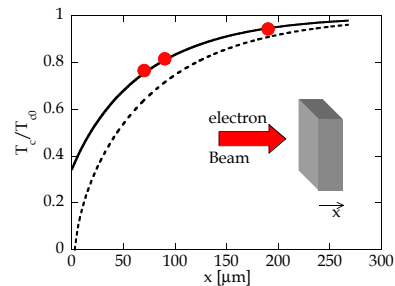


FIG. 3: Dependence of the critical temperature (T_c) normalized to the critical temperature before irradiation (T_{c0}) with the thickness of a sample irradiated with electron a fluence $\Phi = 3.5 \cdot 10^{18} \text{e}^-/\text{cm}^2$. The closed circles are the experimental data measured by resistivity. The solid line is the value expected in function of the depth for an exponential dependence of the rate of defects with the parameters (see text) $\lambda = 80 \mu\text{m}$ and $dT_c/d\Phi = -90 \text{mK}/10^{18} \text{e}^-/\text{cm}^2$. The dashed line is with the parameters $\lambda = 90 \mu\text{m}$ and $dT_c/d\Phi = -115 \text{mK}/10^{18} \text{e}^-/\text{cm}^2$ used for the specific heat fit on figure 2. The inset is a schematic description of the geometry of the irradiation of the samples.

specific heat. On figure 3, the ratio between the critical temperature after and before irradiation with the same fluence for samples of different thickness is reported. The solid curve is $T_c(x)$, where x is the sample thickness, as deduced from equations 1 and 2. The parameters differ slightly than from those of the specific heat fit ($\lambda = 80 \mu\text{m}$ and $\left| \frac{dT_c}{d\Phi}(2.5\text{MeV}) \right| = 90 \text{mK}/10^{18} \text{e}^- \cdot \text{cm}^{-2}$). For comparison, the dashed line shows the expected T_c variation for the resistivity experiment using the parameters of the fit of C_p . However, according to the crudeness of our model, and the difficulties always met in the comparison of T_c between specific heat and resistivity, we believe that it is a "good enough" quantitative agreement. Of course, the lines in figure 3 also represent the distribution of T_c as predicted by our model in a single sample. For the intermediate fluence used in the resistivity experiment, it can be seen that the distribution of T_c is very large and extends very quickly from almost T_{c0} (small change in the T_c onset for a sample 3 times thicker than λ) to 0. The amazing broadening of the specific heat transition is therefore simply explained by a trivial effect of sample geometry and small λ , due to "unlucky" experimental conditions (2.5MeV being too close to the threshold for defect creation).

V. CONSEQUENCES ON THE TRANSPORT MEASUREMENTS

Let us summarize some further consequences on transport measurements. The fact that the Sommerfeld coefficient γ of the normal state specific heat does not depend

on the irradiation shows that the density of states at the Fermi level is not affected. This effect seems to contradict the increase of the quadratic term of the temperature dependence of the resistivity (AT^2) under irradiation (see section I). Indeed A and γ are related by the well known Kadowaki-Woods ratio³³. One can then speculate that the apparent increase of A is an artifact of the distribution of defects. Indeed, when the whole sample is in the normal state, the measured conductivity is an average of the conductivity of the different layers of the sample, which are all in parallel owing to the contact geometry. In the simplest models which assume that the Matthiessen's rule is verified, only the residual resistivity should depend on the impurity concentration. Then, the temperature dependence of the conductivity should be described by :

$$\tilde{\sigma}(T) = \frac{1}{t} \int_0^t \frac{dx}{\rho_0(x) + AT^2} \quad (4)$$

where t is the thickness of the sample, $\rho_0(x)$ the residual resistivity at a depth x , and AT^2 the intrinsic quadratic term, independent of defects concentration. In general the calculation has to be done numerically, however in the limit where AT^2 is small compared to $\rho_0(x)$, the temperature dependence of the resistivity deduced from equation 4 will be of the form $1/\tilde{\sigma}_0 + \tilde{A}T^2$ with :

$$\tilde{\sigma}_0 = \langle \sigma_0 \rangle \quad (5)$$

$$\tilde{A} = A \frac{\langle \sigma_0^2 \rangle}{\langle \sigma_0 \rangle^2} \quad (6)$$

where $\langle \dots \rangle$ is the average over the depth. An increase of the *dispersion* of the defects concentration can therefore be at the origin of an apparent increase of the quadratic temperature dependence. Qualitatively, such an effect is observed with the increase of the thickness of the sample, but also for an increase of the fluence for the same sample.

Quantitatively, since the dependence of the residual resistivity for an infinitely thin sample is proportional to the density of defects, again, a unique parameter $\frac{\partial \rho_{0,i}}{\partial \Phi}$ (where i represents the two different crystallographic orientations) controls the increase of the apparent residual resistivity and of the quadratic term of a thick sample in each direction. At the temperature T , the resistivity at depth x inside the sample irradiated with a fluence Φ is given by:

$$\rho_0(x) = \rho_0 + \frac{\partial \rho_{0,i}}{\partial \Phi} \Phi \exp(-x/\lambda) + AT^2 \quad (7)$$

where ρ_0 is the residual resistivity before irradiation and λ the characteristic length already defined above. The result of this calculation with a parameter $\frac{\partial \rho_{0,i}}{\partial \Phi}$ of 1.4 (resp. 0.6) $\mu\Omega.cm/10^{18}e^-/cm^2$ for a current along

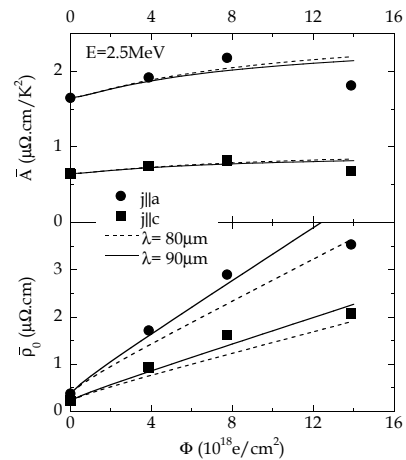


FIG. 4: Dependence of the residual resistivity extrapolated to $T=0K$ (bottom) and of the quadratic temperature dependence of the resistivity (top) for different rates of irradiation for the two samples R4 and R5 of respective crystallographic orientations : current along c-axis and current along a-axis. R4 (squares) is $220\mu m$ thick, and R5 (circles) is $240\mu m$ thick. Lines are the dependence calculated for a rate of defects decreasing exponentially in the thickness of the sample with a characteristic length of $90\mu m$ (plain) or $80\mu m$ (dashed). Only the residual resistivity is assumed to be modified by the defects, with a rate of 1.4 (resp. 0.6) $\mu\Omega.cm/10^{18} \times e^- .cm^{-2}$ for the current along the a (resp. c) direction.

the a-axis (resp. c-axis) is shown on figure 4 for the same sample after different rate of irradiation and on the table 1 for a same fluence on samples of different thickness. The general trend is well described.

Of course, the most interesting transport measurement is the thermal conductivity κ in the superconducting state. The measurements of κ on irradiated samples

Thickness (μm)	$\frac{\rho_0}{\rho_0^{Pure}}$ meas. (Calc.)	$\frac{A}{A^{Pure}}$ meas. (Calc.)
70	9.3 (12)	1.12 (1.03)
90	8.7 (10.6)	1.15 (1.05)
190	6.9 (5.6)	1.30 (1.12)

TABLE I: Ratio after and before irradiation by electrons of energy of 2.5 MeV with a fluence of $3.5 \cdot 10^{18} e^-/cm^2$ of (a) the residual resistivity extrapolated to $T=0K$ and (b) the quadratic temperature dependence of the resistivity. The values measured are compared with the values numerically calculated (between bracket) with an exponential dependence of the concentration of defects in the thickness of the samples. We have also assumed that only the residual resistivity changes (for an homogeneous distribution of defects, see text). The parameters used are $\lambda=80\mu m$ (see text). The parameters used are $\lambda=80\mu m$ (see text) and a variation of the resistivity 1.4 (0.6) $\mu\Omega.cm/10^{18} e^-/cm^2$ in the a (c) direction. These parameters are the same as those used in the figure 4.

reported earlier by our group¹⁹ have been performed on samples typically of several hundreds μm thick. The irradiation parameters were an incident energy of 2.5MeV and a fluence of $3.17 \times 10^{18} \text{e}^-/\text{cm}^2$ and $11 \times 10^{18} \text{e}^-/\text{cm}^2$. The main result was the observation of a dramatic decrease of the thermal conductivity in the superconducting phase and a large increase of the zero temperature extrapolation of κ/T with the fluence of the irradiation. The huge distribution of T_c induced by both irradiations in these experimental conditions (down to $T_c = 0$ K) give a simple and natural explanation to these features. So the question of a "universal limit" in UPt_3 remains completely open, and should be settled by measurements on very thin samples irradiated on both sides to minimize the defects inhomogeneities. From the parameters used in our model, we estimate that for samples $70\mu\text{m}$ thick, irradiated on both faces with total fluences below $1.5 \times 10^{18} \text{e}^-/\text{cm}^2$, the variation of T_c should remain below 20% (from $T_c=0.55$ K before irradiation to 0.46 K after), with an inhomogeneous broadening below 10% of the variation of T_c (i.e. 10 mK which is small compare to the broadening of the "pure" samples). Let us note that for the same experiments performed on the bismuth compounds⁷, the samples were already much thinner ($\approx 20\mu\text{m}$ ³⁴), the transmitted energies twice larger (due to lighter elements) and the threshold energy 4 times smaller³⁵, ensuring that damage was homogeneously distributed through the sample in contrast to the situation encountered for UPt_3 . The same "good" conditions should also be found in the compounds composed of lighter elements like

Cerium based heavy fermion systems or borocarbide superconductors.

VI. CONCLUSION

In conclusion, we have measured and analyzed the specific heat of thick samples of UPt_3 damaged by high-energy electron irradiation. A strong smearing of the specific heat jump at the superconducting transition and a large increase of the residual C/T term are observed. We have shown that a strong dependence of the concentration of defects along the sample thickness can explain quantitatively this feature. Such inhomogeneities have a natural explanation with the heavy elements of UPt_3 . This is further confirmed by the dependence of the critical temperature measured by resistivity with the thickness of the sample. Such macroscopic inhomogeneities give also a natural explanation to the increase of the quadratic term of the temperature dependence of the resistivity, and to the apparent absence of a universal limit in the heat transport measurements reported previously.

We gratefully acknowledge useful discussion with I. Fomin, H. Suderow, V. Mineev and N.E. Hussey. P.R. was partly supported by a Marie Curie Fellowship of the European Community under contract n° HPMF-CT-2000-00954.

-
- ¹ C.J. Pethick and D. Pines; *Phys. Rev. Lett.* **57** 118 (1986)
- ² L.P. Gor'kov and P.A. Kalugin, *Sov. Phys. JETP*, *JETP Lett.* **41** 253 (1984); S. Schmitt-Rink, K. Miyake, C.M. Varma; *Phys. Rev. Lett.* **57** 2575 (1986); P.J. Hirschfeld, P. Wölfe, D. Einzel; *Phys. Rev. B* **37** 83 (1988)
- ³ A.V. Balatsky, M.I. Salkola and A. Rosengren; *Phys. Rev. B* **51** 15547 (1995)
- ⁴ P.A. Lee; *Phys. Rev. Lett.* **71** (1991) 1887.
- ⁵ M.J. Graf, S.K. Yip, J.A. Sauls; *J. Low Temp. Phys.* **114** 257 (1999).
- ⁶ L. Taillefer, B. Lussier, R. Gagnon, K. Behnia, H. Aubin; *Phys. Rev. Lett.* **79** 483 (1997).
- ⁷ S. Nakamae, K. Behnia, L. Balicas, F. Rullier-Albenque, H. Berger and T. Tamegai; *Phys. Rev. B* **63**, 184509 (2001).
- ⁸ M. Suzuki, M.A. Tanatar, N. Kikugawa, Z.Q. Mao, Y. Maeno, T. Ishiguro; *Phys. Rev. Lett.* **88** 7004 (2002).
- ⁹ N.E. Hussey, et al; *Phys. Rev. Lett.* **85** 4140 (2000).
- ¹⁰ K. Hasselbach, L. Taillefer, J. Flouquet; *Phys. Rev. Lett.* **63** 93 (1989).
- ¹¹ G. Bruls, D. Weber, B. Wolf, P. Thalmeier, B. Lüthi, A. de Visser and A. Menovsky, *Phys. Rev. Lett.* **65** (1990), 2294. S. Adenwalla, S.W. Lin, Z. Zhao, Q.Z. Ran, J.B. Ketterson, J.A. Sauls, L. Taillefer, D.G. Hinks, M. Levy and B.K. Sarma ; *Phys. Rev. Lett.* **65** 2298 (1990).
- ¹² for a recent review, see R. Joynt and L. Taillefer, *Rev. Mod. Physics* **74** 235 (2002).
- ¹³ T. Vorenkamp & al; *Phys. Rev. B*, **48** 6373 (1993).
- ¹⁴ Y. Dalichaouch & al; *Phys. Rev. Lett.* **75** 3938 (1995).
- ¹⁵ M.J. Graf, R.J. Keizer, A. de Visser, A.A. Menovsky, J.J.M. Franse; *Phys. Rev. B* **60** 3056 (1999).
- ¹⁶ A. de Visser; *Physica B* **319** 233 (2002) and references therein.
- ¹⁷ J.P. Brison, N. Keller, P. Lejay, J.L. Tholence, A. Huxley, N. Bernhoeft, A.I. Buzdin, B. Fåk, J. Flouquet, L. Schmidt, A. Stepanov, R.A. Fisher, N. Phillips and C. Vettier, *J. Low Temp. Phys.* **95** 145 (1994).
- ¹⁸ J.B. Kycia & al; *Phys. Rev. B* **58** R603 (1998).
- ¹⁹ H. Suderow, S. Kambe, J.P. Brison, A.D. Huxley, J. Flouquet, F. Rullier-Albenque; *J. Low Temp. Phys.* **116** 393 (1999).
- ²⁰ B. Lussier, B. Ellman, L. Taillefer, *Phys. Rev. Lett.* **73** (1994), 3294; *Phys. Rev. B* **53** (1996), 5145.
- ²¹ H. Suderow, J.P. Brison, A.D. Huxley, J. Flouquet; *J. Low Temp. Phys.* **108** 11 (1997); *Phys. Rev. Lett.* **80** 165 (1998).
- ²² J.P. Brison, H. Suderow, P. Rodière, A. Huxley, S. Kambe, F. Rullier-Albenque, J. Flouquet; *Physica B* **281-282** 872 (2000).
- ²³ I.A. Fomin; *Pis'ma Zh. Eksp Teor. Fiz* **72** 94 (2000); *JETP-*

- Letters **72** 66 (2000).
- ²⁴ D. Gosset; Rapport CEA-R-5381 (1987).
- ²⁵ L. Pages, E. Bertel, H. Joffre, L. Sklavenitis, Rapport CEA-R-3941 (1970).
- ²⁶ E.A. Schuberth, M. Fisher, Physica B **194-196** 1983 (1994).
- ²⁷ P. Vajda; Rev. Mod. Phys. **49** 481 (1977).
- ²⁸ F. Rullier-Albenque, P.A. Vieillefond, H. Alloul, A.W. Tyler, P. Lejay, J.F. Marucco; Europhysics Lett. **50** 81 (2000).
- ²⁹ P.A. Mc Kenzie, R.K.W. Haselwimmer, A.W. Tyler, G.G. Lonzarich, Y. Mori, S. Nishizaki, Y. Maeno; Phys. Rev. Lett. **80** 161 (1998).
- ³⁰ A.A. Abrikosov, L.P. Gor'kov; Zh. Eksperim. i Teor. Fiz **39** (1960) 1781; Soviet Phys. - JETP **12** 1243 (1961). A.A. Abrikosov; Physica **C 214** 107 (1993).
- ³¹ A.I. Larkin; Pis'ma Zh. Eksp Teor. Fiz **2** (1965) 205; JETP Lett. **2** 130 (1965).
- ³² G. Yang, K. Maki; Eur. Phys. J. B **21** 61 (2001).
- ³³ K. Kadowaki, S.B. Woods; Solid State Comm. **58** (1986) 507.
- ³⁴ K. Behnia, private communication.
- ³⁵ F. Rullier-Albenque, A. Legris, H. Berger and L. Forro; Physica **C 254** 88 (1995); A. Legris, F. Rullier-Albenque, E. Radeva and P. Lejay; J. Phys. **I France 3** 1605 (1993).